

DISPERSION ERRORS OF B-SPLINE BASED FINITE ELEMENT METHOD IN ONE-DIMENSIONAL ELASTIC WAVE PROPAGATION

Radek Kolman¹, Jiří Plešek¹, Miloslav Okrouhlík¹ and Dušan Gabriel¹

¹Institute of Thermomechanics
Academy of Sciences of the Czech Republic
Dolejšková 5
182 00 Praha 8, Czech Republic
e-mail: {kolman,plesek,ok,gabriel}@it.cas.cz

Keywords: Wave Propagation, Dispersion Analysis, B-spline based finite element method.

Abstract. *The spatial discretization of elastic continuum by finite element method (FEM) introduces dispersion errors to numerical solutions of wave propagation tasks. For higher order Lagrangian as well as Hermitian elements there are optical modes in their frequency spectra leading to spurious oscillations of shock induced responses in a vicinity of propagating wavefronts. Furthermore, the behavior of classical higher order elements accounts for discontinuities in their spectra as well as for false representation of maximum frequency, the error of which increases with element order. For brevity this property is called the divergent behavior in the text. The recent innovations in finite element analysis rely on spline-based shape functions, taking inspiration in CAD (Computer Aided Design) approaches where the B-splines and mainly NURBS (non-uniform rational B-spline) representations are regularly employed. B-spline as well as NURBS curves are piecewise polynomial curves that are differentiable up to a prescribed order. The B-splines functions, employed as finite element shape functions, are examined in this paper, using the 1D stress wave modeling as a testing vehicle. It is shown that the employed approach leads to substantial minimization of dispersion errors; furthermore the errors decrease with increasing order of B-spline elements. It is believed that the B-spline based FE technology represents a promising tool allowing to increase reliability of numerical solutions of wave propagation problems.*

1 INTRODUCTION

The numerical solution of fast transient elastodynamics problems by the classical Lagrangian as well as Hermitian type of the finite element method (FEM) [1] is influenced by dispersion errors caused by both spatial and temporal discretizations [2]. A monochromatic harmonic stress wave propagates in unbounded elastic continuum regardless of its frequency and correspondingly a wave packet propagates without distortion. When these propagating phenomena are modeled by FEM the speed of a single harmonic wave depends on its frequency and thus a wave packet is distorted. The parasitic effects do not exist in 'ideal' unbounded continuum. The dispersive properties of one-dimensional Lagrangian and Hermitian elements were studied in Ref. [3]. Furthermore, the finite element (FE) mesh behaves as a frequency filter - higher frequencies are transferred with a strong attenuation.

The theoretical basis of the dispersion analysis of FEM for the solution of the hyperbolic partial differential equation has been laid in [4], where the Gibb's effect with the connection of FEM was observed. The oscillations near the wavefront or the stress jump change do not vanish for the fine-grained mesh. Fourier method as the dispersion analysis tool of the numerical solution of the hyperbolic partial differential equation is described in [5]. Very simple and efficient computational strategy of the complex wavenumber Fourier analysis of FEM is presented in Ref. [6].

In seismology the spectral finite elements [7] appeared recently. Spectral finite elements are of h-type finite elements, where nodes have special positions along the elements corresponding to the numerical quadrature schemes. But the displacements along element are approximated by the Lagrangian interpolation polynomials. The spectral finite elements improve dispersion errors for lower dispersion branches but not for upper ones.

A modern approach in the finite element analysis is the isogeometric analysis [8], where shape functions are based on varied types of splines. For example, Bézier representation, B-spline (basis spline), NURBS (non-uniform rational B-spline), PB-spline, T-spline and others are used for spatial discretization. This approach has an advantage that the geometry and approximation of the field of unknown quantities is prescribed by the same technique. Another benefit is that the approximation is smooth.

Dispersion of B-spline based finite elements was established for the same recurrent (uniform) B-spline basis functions [5] approximating one dimensional infinite domain. It was shown, that the optical modes did not exist and next, dispersion errors were reported to decrease with increasing order of B-spline shape functions [9]. This is a very good result for the explicit dynamics, where critical time step is bounded by the highest eigenfrequency of the whole system [10].

Generally, the B-spline or NURBS basis functions for bounded solids are not uniform. For this reason, the non-homogeneity of basis functions near the boundary of the domain produces the dispersion and attenuation behavior. These behavior can be controlled by parameterization of B-spline entity, by order of piecewise polynomials, etc. In this paper, the dispersion of B-spline based finite element will be determined for a one-dimensional elastic wave propagation problem. Numerical parameters of B-spline representation will be tested to show their dispersion and attenuation.

2 PROPAGATION OF ELASTIC WAVES IN ONE-DIMENSIONAL CASE

In one-dimensional case the classical equation governing linear elastic wave propagation [11] is given by

$$c_0^2 \frac{\partial^2 u}{\partial x^2} - \frac{\partial^2 u}{\partial t^2} = 0, \quad \text{where } x \in (-\infty, \infty), t \in [0, \infty), \quad (1)$$

where c_0 denotes the wave propagation speed, $u(x, t)$ is the displacement field, x is the position and t is the time. The unbounded one-dimensional continuum is assumed, therefore boundary conditions are not prescribed. The 1D continuum can be realized as a 'thin' elastic bar, the material of which is characterized by Young's modulus E and mass density ρ . For a 'thin' elastic bar, the wave speed is given by $c_0 = \sqrt{E/\rho}$. In case of constant E and ρ , the wave speed is as well constant. Moreover, the value of wave speed is independent of the wavenumber or frequency of wave. This continuum is called non-dispersive [11].

3 B-SPLINE BASED FINITE ELEMENT METHOD

Firstly, the B-spline basis functions will be mentioned, see details in Ref. [12]. For a given knot vector Ξ , the B-spline basis functions are defined recursively starting with piecewise constants ($p = 0$)

$$N_{i,0}(\xi) = \begin{cases} 1 & \text{if } \xi_i \leq \xi \leq \xi_{i+1}, \\ 0 & \text{otherwise.} \end{cases} \quad (2)$$

The basis functions $N_{i,0}(\xi)$ are step functions, equal to zero everywhere except on the half-open interval $\xi = [\xi_i, \xi_{i+1})$, where ξ is parameter usually chosen so, that $\xi = [0, 1]$.

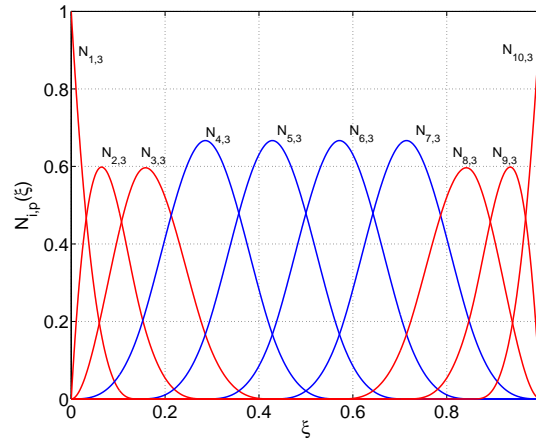


Figure 1: Example of cubic B-spline basis functions for ten control points $n = 10$ and uniform knot vector Ξ . Red lines correspond to non-uniform basis functions and blue lines correspond to uniform (homogeneous) basis functions. The number of non-uniform basis functions depends on the polynomial order.

For $p = 1, 2, 3, \dots$, they are defined by

$$N_{i,p}(\xi) = \frac{\xi - \xi_i}{\xi_{i+p} - \xi_i} N_{i,p-1}(\xi) + \frac{\xi_{i+p+1} - \xi}{\xi_{i+p+1} - \xi_{i+1}} N_{i+1,p-1}(\xi). \quad (3)$$

This is referred to as the Cox-de Boor recursion formula [12]. A knot vector in one dimensional case is a non-decreasing set of coordinates in the parameter space, written $\Xi = \{\xi_1, \xi_2, \dots, \xi_m\}$,

where $\xi_i \in R$ is the i -th knot, i is the knot index, $i = 1, 2, \dots, m$, where $m = n + p + 1$, p is the polynomial order, and n is the number of basis functions used to construct a B-spline curve. Equation (3) can yield the quotient $0/0$, for this case the quotient is prescribed zero. The main properties of $N_{i,p}$, defined by (2) and (3), are introduced in Ref. [12]. Example of cubic B-spline basis functions for ten control points $n = 10$ and uniform knot vector is displayed in Fig. 1.

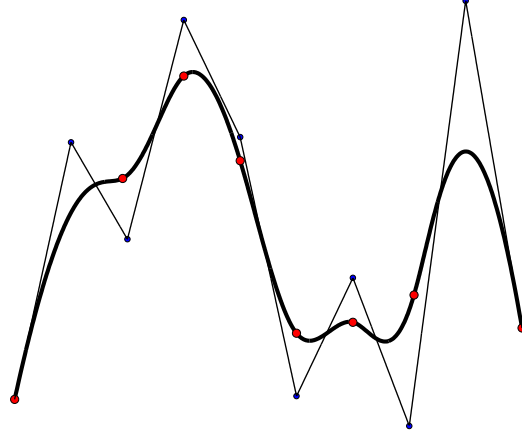


Figure 2: Example of cubic B-spline curve for ten control points and uniform knot vector. The corresponding control polygon is depicted.

In CAD technology [13] a B-spline curve is given by linear combination of B-spline basis functions $N_{i,p}$ [12]

$$\mathbf{C}(\xi) = \sum_{i=1}^n N_{i,p}(\xi) \mathbf{B}_i, \quad (4)$$

where $\mathbf{B}_i, i = 1, 2, \dots, n$ are corresponding control points. Piecewise linear interpolation of control points gives the so-called control polygon. Example of cubic B-spline curve with its control polygon is shown in Fig. 2.

The open B-spline curve interpolating end points is used, where the knot vector is prescribed as

$$\Xi = \{a, \dots, a, \xi_{p+2}, \dots, \xi_n, b, \dots, b\}, \quad (5)$$

where values are usually set as $a = 0$ and $b = 1$. The multiplicity of the first and last knot value is $p + 1$. If the values ξ_{p+1} up to ξ_{n+1} are chosen uniformly, the knot vector Ξ is called uniform knot vector, otherwise non-uniform, for more details see Ref. [12]. The B-spline curve for the knot vector given by (5) is passed through the end points of the control polygon.

Analogically, the spatial coordinate for a one-dimensional continuum can be approximated by linear combination of B-spline basis functions $N_{i,p}$

$$x(\xi) = \sum_{i=1}^n N_{i,p}(\xi) x_i^{\mathbf{B}}, \quad (6)$$

where $x_i^{\mathbf{B}}, i = 1, 2, \dots, n$ are positions of control points in the x-direction. Furthermore, the approximation of the displacement field u^h by the B-spline approach is given by

$$u^h(\xi) = \sum_{i=1}^n N_{i,p}(\xi) u_i^{\mathbf{B}}, \quad (7)$$

where u_i^B is the component of the vector of control variables – displacements corresponding to the control points.

A scheme of a admissible dependence of a one dimensional displacement field based on B-spline representation is presented in Fig. 3. Generally, the displacement field discretized by B-spline technology in one-dimensional case can be controlled by following parameters:

- length of element patch h (*h-refinement*),
- polynomial order p (*p-refinement*),
- number of control points n (*k-refinement*),
- positions of control points x_i^B , $i = 1, 2, \dots, n$, (choice of parameterization),
- components of the knot vector Ξ and their multiplicities,
- continuity between patches C^m , $m \leq p - 1$ order of continuity.

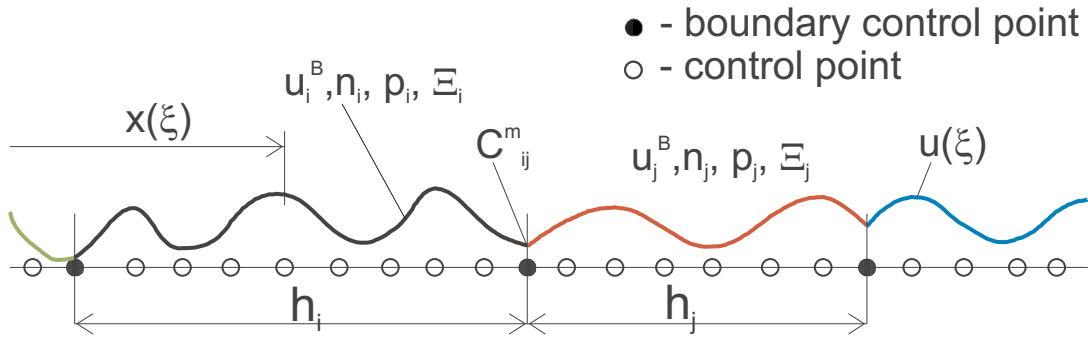


Figure 3: Scheme for permissible spatial discretization of a one-dimensional domain by B-spline based FE. h_i denotes a length of B-spline segment, u_i^B are control variables, n_i is number of control points, p_i denotes polynomial order, Ξ_i denotes a knot vector for i -th B-spline segment. C_{ij}^m marks order of continuity between i -th and j -th B-spline segment. Spatial coordinate $x(\xi)$ and corresponding displacement $u(\xi)$ are parametric functions of parameter ξ .

In this paper, C^0 continuity between B-spline segments with the identical length h is considered. The number of control points n , their positions and polynomial order p are the same. The knot value appears only once in the knot vector, but the first and last knot values appear $p + 1$ times. Of course, the continuity of the displacement field inside the B-spline segment is C^{p-1} .

In the following text, the continuous Galerkin's approximation method [1] for the solution of partial differential equations is employed. Spatial discretization of elastodynamics problems by finite elements leads to the second order ordinary differential system in the form [1]

$$\mathbf{M}\ddot{\mathbf{u}} + \mathbf{K}\mathbf{u} = \mathbf{R}. \quad (8)$$

Here, \mathbf{M} is the mass matrix, \mathbf{K} the stiffness matrix, \mathbf{R} is the time-dependent load vector, \mathbf{u} and $\ddot{\mathbf{u}}$ contain nodal displacements and accelerations. Neglecting the loading we have $\mathbf{R} = \mathbf{0}$. A lot of discrete time direct integration methods for the system (8) were developed [1]. However, the time is considered continuous in this work.

The element mass and stiffness matrices are given by

$$\mathbf{M}^e = \int_{h^e} \rho \mathbf{H}^T \mathbf{H} \, dx \quad (9)$$

and

$$\mathbf{K}^e = \int_{h^e} E \mathbf{B}^T \mathbf{B} \, dx \quad (10)$$

where h^e denotes the finite element length or length of B-spline segment, \mathbf{B} is the strain-displacement matrix, \mathbf{H} stores the displacement interpolation (shape) functions h_i [1]. For case of B-spline based FEM, shape functions are denoted $N_{i,p}$. Integrations (9) and (10) are carried over the element domain. If the theory of linear elastodynamics is considered, then mass matrix \mathbf{M}^e (9) and stiffness matrix \mathbf{K}^e (10) are constant. Global matrices are assembled in the usual fashion. Mass matrix defined by (9) is called consistent mass matrix and this mass matrix is employed in the following text. The stiffness matrix \mathbf{K} and mass matrix \mathbf{M} is computed numerically by the Gauss-Legendre quadrature formula [1].

4 DISPERSION ANALYSIS

The complex wavenumber dispersion analysis was performed for one-dimensional finite elements in Ref. [6]. In Fourier analysis [5], the displacement u_i^h corresponding to given spatial discretization is prescribed in the form of wave solution

$$u_i^h = A_i e^{i(\omega t - \psi^h x_i)}, \quad (11)$$

where A_i is displacement amplitude, ω is angular velocity, imaginary unit $i = \sqrt{-1}$ and x_i is the position. The discrete (numerical) wavenumber k^h equals to the real part of ψ^h , $k^h = \text{Re } \psi^h$. Imaginary part $b^h = \text{Im } \psi^h$ has a physical meaning of the attenuation intensity.

In Fourier analysis, the assumed solution of (11) is inserted to the equation (1) and the dispersion relation $\omega = f(k^h)$ is obtained. The dispersion errors can be measured by non-dimensional numerical phase speed c^h/c_0 , where numerical phase speed is defined by the relationship $c^h = \omega/k^h$. Mostly, the dispersion errors are depicted as a function of the non-dimensional numerical wavenumber $k^h h$, where h is characteristic length of finite element domain or B-spline segment.

5 RESULTS OF DISPERSION ANALYSIS FOR B-SPLINE BASED FEM

In this section, the dispersion diagrams for B-spline based FEM are shown for different number of control points with linear or non-linear parameterization and for different polynomial order, respectively. These graphs are compared with results for classical Lagrangian finite elements.

5.1 Uniform B-spline FEM versus classical finite element

Dispersion of one-dimensional Lagrangian FE was been studied in [3], [6]. The normalized dispersion errors in phase speed are depicted in Fig. 4 (on the left). These errors are divergent with the polynomial order of approximation of a displacement field. In Fig. 4 (on the left), h denotes the length of Lagrangian finite element. Nevertheless, the distances between uniformly-spaced nodes are h/p . The wavenumbers are normalized, being divided by appropriate polynomial order p . Thus, the non-dimensional numerical wavenumbers are in the range $k^h h/p = [0, \pi]$. The horizontal jumps in the dispersion graph on Fig. 4 (on the left) correspond to the attenuating solution [14]. For higher order Lagrangian finite elements, the optical modes are

occurred [2]. These vibration modes produce the spurious oscillations in numerical solutions of transient elastodynamics problems.

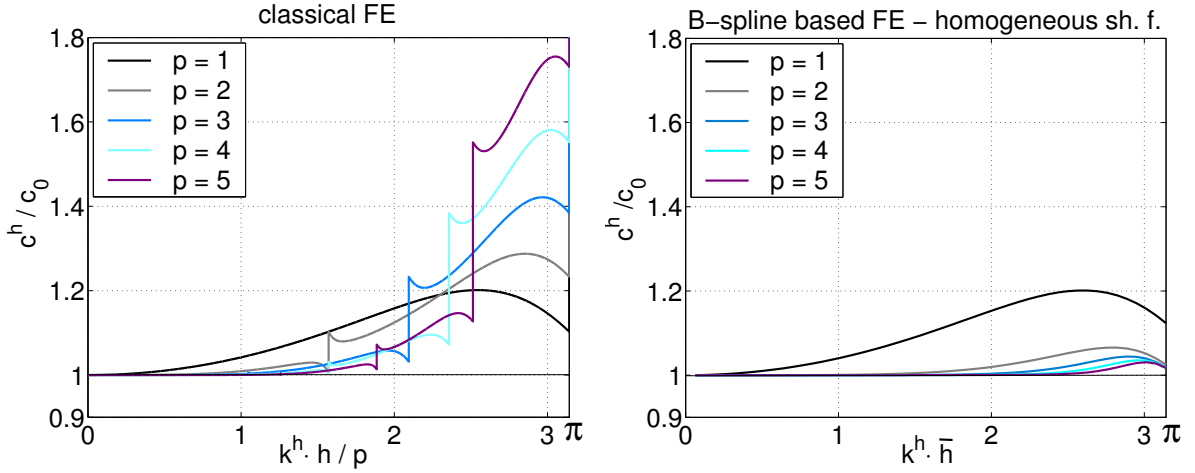


Figure 4: Dispersion errors for Lagrangian FE (on the left) [3], [6] and B-spline based FE (on the right) [9] for different polynomial order p . h denotes the finite element length, \bar{h} is the distance of uniformly-spaced control points.

In Ref. [8], the errors of eigenfrequency of an elastic fixed-fixed bar computed by classical FEM and B-spline based FEM are compared. The dependence of eigenfrequency ω^h/ω on the corresponding counter has the same character as the dependence c^h/c_0 on the corresponding non-dimensional wavenumber $k^h h$. It is a consequence of the duality principle accomplished in Ref. [9].

The dispersion analysis of B-spline based FEM has been investigated in Ref. [5], where uniform basis shape functions are employed. This case is in agreement with a model of an infinite elastic 'thin' bar. The dispersion graph for uniform B-spline based FEM is presented in Fig. 4 (on the right), where the high mode behavior is convergent with the polynomial order p of B-spline approach. The dispersion errors are decreasing with increasing polynomial order. The permissible values of numerical wavenumber $k^h \bar{h}$ are in the range $[0, \pi]$. In Fig. 4 (on the right), \bar{h} denotes distance of uniformly-spaced control points. The optical modes and attenuating solution in the right-open range $k^h \bar{h} = [0, \pi)$ do not exist, but for $k^h \bar{h} = \pi$ the attenuating solution arises. The spatial resolution limit corresponds to the numerical wavenumber is $k^h \bar{h} = \pi$, where positions of control points are in the 'saw tooth' oscillation form. The uniform B-spline based finite element for discretization of a one-dimensional domain produces better dispersion dependence without optical modes and band gaps [14] with respect to the Lagrangian classical FEM [9].

REMARK: Another solution of wave equation (1) discretized by uniform B-spline based FEM exists [9]. This solution is called evanescent solution [14]. This solution of discretized system is characteristic by non-zero imaginary parts of ψ^h and for the numerical wavenumber is valid $k^h \bar{h} \neq i\pi, i = 0, 1, 2, \dots, p$, simultaneously. The number of the evanescent solutions is $p-1$, see Ref. [9]. The evanescent solutions do not have practically meaning in the numerical solution of wave equation due to their attenuating effect.

5.2 Non-linear parameterization - uniformly-spaced control points

This section deals with the dispersion analysis for B-spline segments with polynomial order p , different number of uniformly-spaced control points. And also with the uniform knot vector and for case, where individual B-spline segments are connected only with C^0 continuity with their neighbouring B-spline segments. In Fig. 5 (on the left), dispersion errors c^h/c_0 of the quadratic ($p = 2$) B-spline based FE are drawn. In Fig. 5 (on the right) there are presented the dispersion errors for cubic ($p = 3$) B-spline based FE with different number of control points, where h denotes the patch length of B-spline (see Fig. 3). For increasing number of control points, the dispersion errors are convergent to value of wave speed c_0 – i.e. to the exact solution for continuum.

The vertical jumps pertain to the decay solution with non-zero attenuation. These parts of the dispersion dependencies depict quantitatively the passing and band gaps in the frequency range [14]. Thereby, the band gaps exist also for the B-spline based element method with C^0 continuity between B-spline segments. With increasing number of control points the band gap range is decreasing and the maximal band gap range occurs in higher dispersion branches. It can be shown, that dispersion errors are influenced by shape (basis) functions $N_{i,p}$ defined in the vicinity of patch domain boundary, see Fig. 1. The corresponding shape functions are not homogeneous due the interpolation of end points [12].

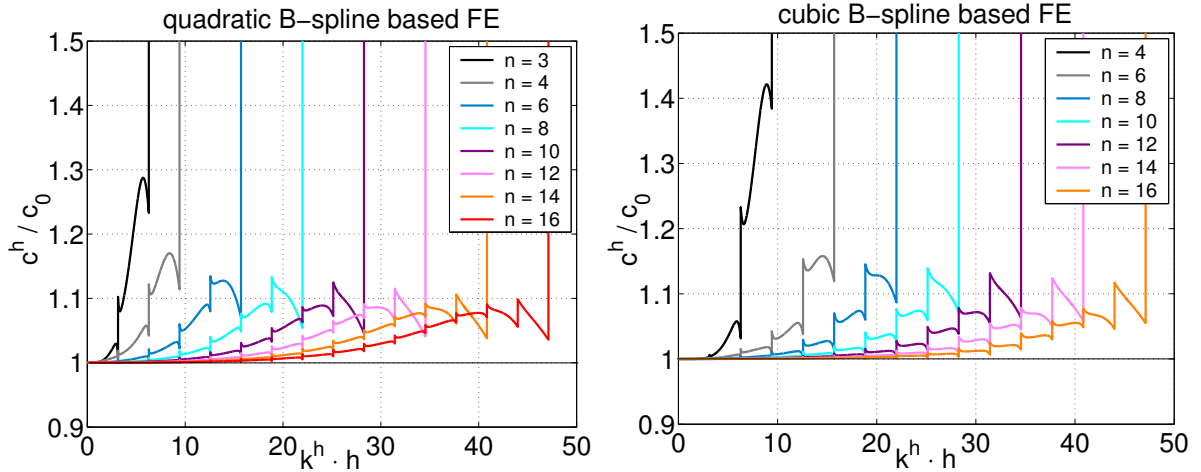


Figure 5: Dispersion errors for quadratic (on the left) and cubic (on the right) B-spline based FE with different number of control points. The red line corresponds to homogeneous shape functions [9].

The dispersion dependencies in Fig. 5 can be redrawn to the normalized non-dimensional wavenumber $k^h h / (n - 1)$. Which means that the abscissa variables are divided by the appropriate number of distances of control points, i.e. $n - 1$. The distance between uniformly-spaced control points is $\bar{h} = h / (n - 1)$. It is the averaged distance of control points. The normalized numerical wavenumbers are in the range $k^h h / (n - 1) \in [0, \pi]$. The normalized dispersion errors are depicted in Fig. 6, where corresponding dispersion errors for uniform B-spline shape functions (Fig.4 (on the right)) are added. The normalized dispersion errors for quadratic B-spline are shown in Fig. 6 (on the left) and for cubic B-spline are represented in Fig. 6 (on the right). For clarity the number of control points in Fig. 6 is different from that appearing in Fig. 5. It is of interest that the mentioned normalized dispersion errors are approaching to those of the uniformly (homogeneous) B-spline shape functions (Fig. 4).

For minimization of dispersion errors, the increasing number of control points (*k-refinement*) is better than the partition of the B-spline segments (*h-refinement*). The higher order of continuity inside the B-spline produces more reliable dispersion behavior.

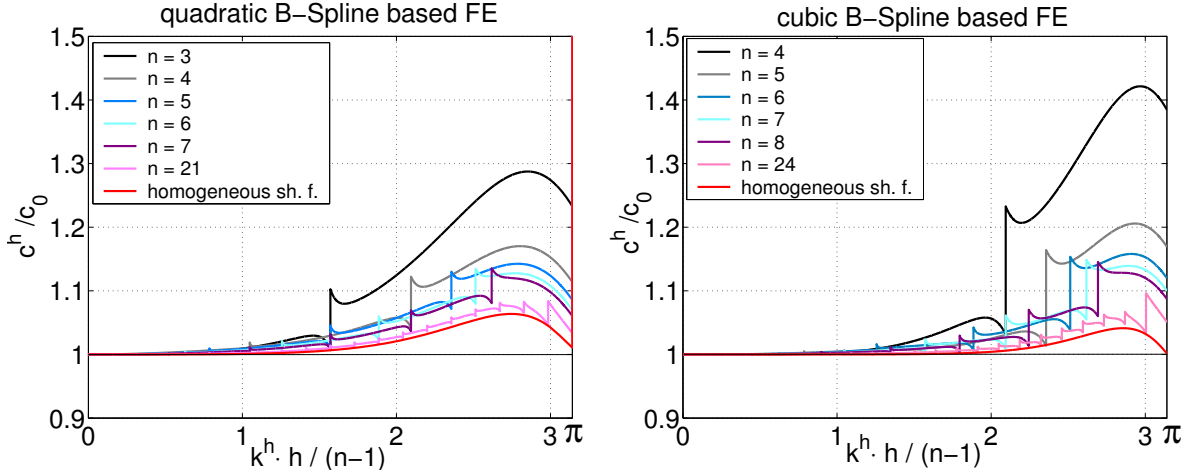


Figure 6: Normalized dispersion errors for quadratic (on the left) and cubic (on the right) B-spline based FE with different number of control points. The red line corresponds to homogeneous shape functions [9].

REMARK: For situations, where number of control points is $n = p + 1$ and B-spline segments are only connected with C^0 continuity, the dispersion dependencies are identical with those of Lagrangian finite elements (Fig. 4 (on the left)).

5.3 Linear parameterization - Graville abscissa

The simple modification of the previously shown B-spline non-linear parameterization is based on a choice of special positions of control points. Good interpolation properties of B-splines can also be obtained by so called Graville abscissa. In such a case the abscissa is associated with the knot vector Ξ . See [15] and [16] for details. Thus, the control points are given by the formula

$$x_i^*(\xi) = \frac{\xi_{i+1} + \dots + \xi_{i+p}}{p}, \quad i = 1, 2, \dots, n. \quad (12)$$

The set of control points positions obtained this way (12) is usually called the set of averaged collocation points or Greville collocation points. If the knot vector is chosen so, that $a = 0$, $b = 1$ in (5) and the outside knots are with $p + 1$ multiplicity, then the boundary control points are located on $x_1^* = 0$ and $x_n^* = 1$. B-spline displacement field is passed through end points. Therefore, the coordinates $x_i, i = 1, 2, \dots, n$ of control points of B-spline segment with length h are given by

$$x(\xi) = x_i^*(\xi) \cdot h. \quad (13)$$

The fundamental property of this parameterization based on the Greville abscissa is such, that Jacobians of the transformation from the parametric space to the physical space are constant for arbitrary parameter ξ , i.e. $\frac{dx(\xi)}{d\xi} = \text{const}$ for $\forall \xi \in [0, 1]$ [16]. This parameterization is called linear.

The normalized dispersion errors c^h/c_0 versus non-dimensional wavenumber $k^h h / (n - 1)$ for quadratic B-spline with linear parameterization are shown in Fig. 7 and for cubic B-spline

with linear parameterization are in Fig. 8, where influence of the number of control points is displayed. The dispersion graphs are normalized with respect to the averaged distance between the control points prescribed by relationship (12) and (13), respectively. The details of $c^h - k^h$ -curves presented in Figs. 7 (on the left) and 8 (on the left) are enlarged in Figs. 7 (on the right) and 8 (on the right). The band gap ranges for this parameterization are rapidly disappearing.

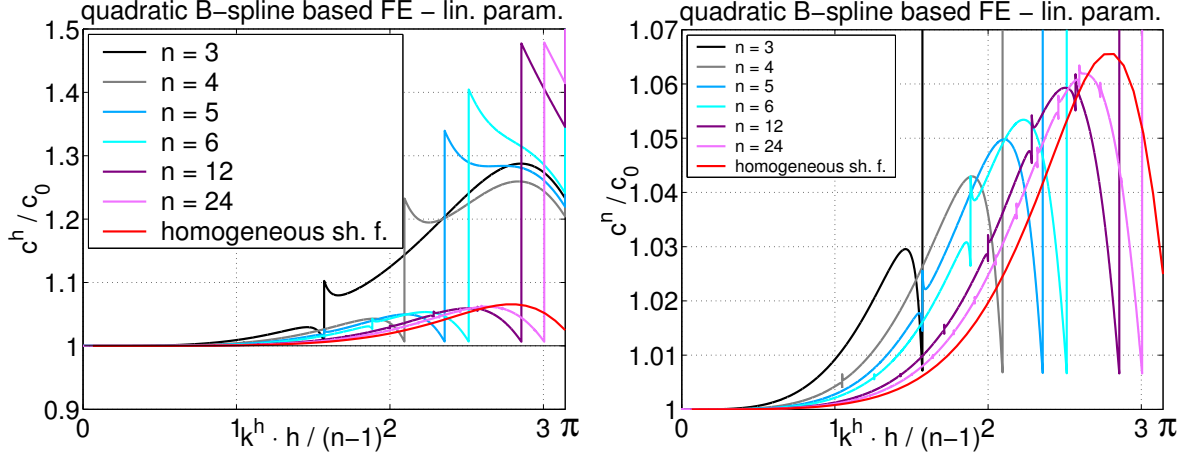


Figure 7: Normalized dispersion errors for quadratic B-spline based FE with linear parameterization. The red line corresponds to homogeneous shape functions [9].

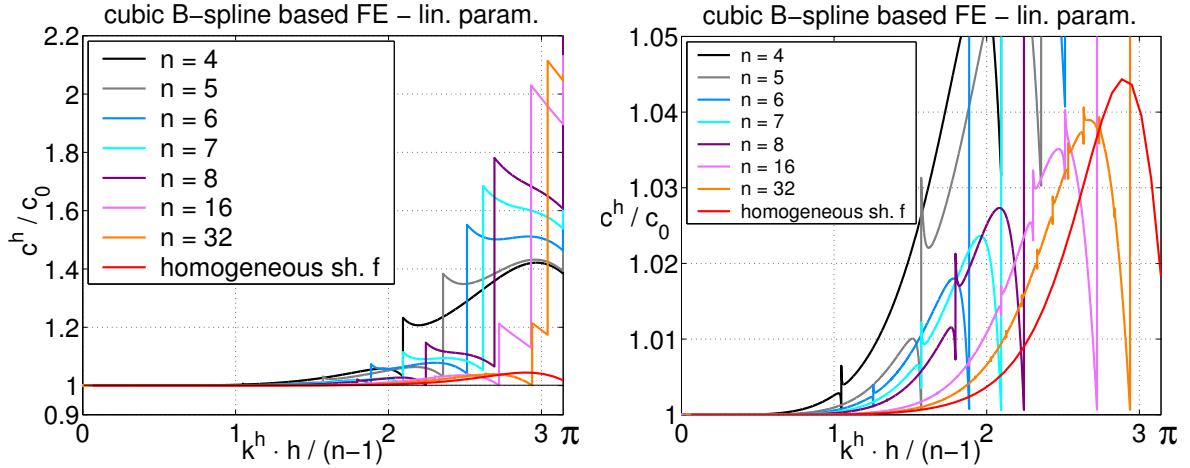


Figure 8: Normalized dispersion errors for cubic B-spline based FE with linear parameterization. The red line corresponds to homogeneous shape functions [9].

The dispersion curves for linear parameterization converge to the solution employing uniform (homogeneous) B-spline basis functions. For large number of control points, approximately $n \geq 10$, the $p - 1$ highest dispersion branches ω versus k^h display a constant behavior. From it follows that the group speed $c_g^h = d\omega/dk^h = 0$ and the dependence of phase speed $c^h = \omega/k^h$ is a linear function with the negative slope. The wave corresponding to the last $p - 1$ dispersion branches are not propagated through a elastic bar discretized by B-spline approach. The linear parameterization rapidly minimize the dispersion errors. The maximal error in phase speed for quadratic B-spline discretization is less than 7% and for cubic B-spline less than 4% thanks to the linear parameterization. This is very good property of B-spline based finite element method for case, where connection between several B-spline segments are only C^0 .

6 CONCLUSIONS

It was shown that the dispersion errors of B-spline based finite element method for increasing number of control points converge to the continuum solution. The solution with high number of control points is near by the solution for uniform B-spline shape functions. On the other hand, its dependence is with jumps from the reason of existing of passing and band gaps. Moreover, the spurious modes are reduced by the B-spline based spatial discretization thanks to higher order of continuity of approximation of a unknown quantity (in this case displacement). Further, the dispersion errors and ranges of band gaps can be similarly eliminated by a special choice of positions of control points, for example, by the Greville abscissa. It is valid as well in the case, where individual B-spline segments are only connected with C^0 continuity. B-splines basis functions as shape functions have a potential for using in high performance and accurate finite element analysis of elastic wave propagation problems.

Acknowledgment

This work was supported by the grant projects GA ČR P101/10/P376, 101/09/1630, 101/07/1471 and P101/11/0288 under AV0Z20760514.

REFERENCES

- [1] T.J.R. Hughes, *The Finite Element Method: Linear and Dynamic Finite Element Analysis*. New York: Prentice-Hall, Englewood Cliffs, 1983.
- [2] T. Belytschko, R. Mullen, On dispersive properties of finite element solutions. J. Miklowitz eds. *Modern Problems in Elastic Wave Propagation*, John Wiley, 67–82, 1978.
- [3] M. Okrouhlík, C. Höschl, A contribution to the study of dispersive properties of one-dimensional Lagrangian and Hermitian elements. *Computers & Structures*, **49**(5), 779–795, 1993.
- [4] R.C.Y. Chin, Dispersion and Gibb’s phenomenon associated with difference approximations to initial boundary-value problems. *J. Comp. Phys*, **18**, 233–247, 1975.
- [5] R. Vichnevetsky, J.B. Bowles, *Fourier analysis of numerical approximations of hyperbolic equations*. SIAM, Philadelphia, 1982.
- [6] L.L. Thompson, P.M. Pinky, Complex wave-number Fourier-analysis of the p-version finite element method. *Computational Mechanics*, **13**(4), 255–275, 1995.
- [7] G. Seriani, S.P. Oliveira, Dispersion analysis of spectral element methods for elastic wave propagation. *Wave Motion*, **45**(6), 729–744, 2008.
- [8] J.A. Cottrell, T.J.R. Hughes, Y. Bazilevs, *Isogeometric Analysis: Toward Integration of CAD and FEA*. John Wiley & Sons, New York, 2009.
- [9] T.J.R. Hughes, A. Reali, G. Sangalli, Duality and Unified Analysis of Discrete Approximations in Structural Dynamics and Wave Propagation: Comparison of p-method Finite Elements with k-method NURBS. *Comput. Methods Appl. Mech. Engrg.*, **197**, 4104–4124, 2008.

- [10] K.C. Park, Practical aspect of numerical time integration. *Computers & Structures*, **7**, 343–353, 1977.
- [11] H. Kolsky, *Stress Wave in Solids*. New York: Dover Publications, 1963.
- [12] L. Piegl, W. Tiller, *The NURBS Book, (Monographs in Visual Communication), Second Edition*. Springer-Verlag, 1997.
- [13] G. Farin, *Curves and Surfaces for CAGD, A Practical Guide, Fifth Edition*. Morgan Kaufmann Publishers, 1999.
- [14] L. Brillouin, *Wave propagation in Periodic Structures: Electric Filters and Crystal Lattices*. New York: Dover Publications, 1953.
- [15] T.N.E. Greville, On the normalization of the B-splines and the location of the nodes for the case of unequally spaced knots. O. Shiska eds. *Inequalities*, Academic Press, New York, 1967
- [16] H. Prautzsch, W. Boehm and M. Paluszny, *Bézier and B-Spline Techniques*. Springer Berlin Heidelberg, 2010.